Monthly Notices
of the
ROYAL ASTRONOMICAL SOCIETY

Mon. Not. R. Astron. Soc. **420,** 1541–1552 (2012) doi:10.1111/j.1365-2966.2011.20139.x

Inner dusty regions of protoplanetary discs – I. High-resolution temperature structure

Dejan Vinković★

Physics Department, University of Split, Nikole Tesle 12, HR-21000 Split, Croatia

Accepted 2011 November 3. Received 2011 November 2; in original form 2011 September 7

ABSTRACT

Our current understanding of the physical conditions in the inner regions of protoplanetary discs is being increasingly challenged by more detailed observational and theoretical explorations. The calculation of the dust temperature is one of the key features that we strive to understand and this is a necessary step in image and flux reconstruction. Here, we explore the coexistence of small (0.1-μm radius) and large (2-μm radius) dust grains, which can coexist at distances from the star where small grains would not survive without large grains shielding them from the direct starlight. Our study required a high-resolution radiative transfer calculation, which is capable of resolving the large temperature gradients and disc-surface curvatures caused by dust sublimation. This method of calculation was also capable of resolving the temperature inversion effect in large grains, where the maximum dust temperature is at a visual optical depth of $\tau_V \sim 1.5$. We also show disc images and spectra, with disentangled contributions from small and large grains. Large grains dominate the near-infrared flux, mainly because of the bright hot inner disc rim. Small grains populate almost the entire interior of the inner disc, but they appear at the disc's surface at distances 2.2 times larger than the closest distance of the large grains from the star. Nevertheless, small grains can contribute to the image surface brightness at smaller radii because they are visible below the optically thin surface defined by stellar heating. Our calculations demonstrate that the sublimation temperature does not provide a unique boundary condition for radiative transfer models of optically thick discs. The source of this problem is the temperature inversion effect, which allows the survival of optically thin configurations of large grains closer to the star than the inner radius of the optically thick disc. Future attempts to derive more realistic multigrain inner disc models will need the numerical resolution shown in our study, especially if the dust dynamics is considered where grains can travel through zones of local temperature maxima.

Key words: radiative transfer – protoplanetary discs – circumstellar matter – stars: imaging – stars: pre-main-sequence.

1 INTRODUCTION

A pressing issue, which has been raised by the ongoing prolific discoveries of extrasolar planets, is the identification of the conditions under which planets form and develop. A general scenario invokes a circumstellar (protoplanetary) disc of dust and gas around young pre-main-sequence stars, where planets are expected to form. The advancements in observational and theoretical techniques over recent decades have enabled extensive explorations of the evolution of these discs (Williams & Cieza 2011). One of the key issues in the exploration of protoplanetary discs is understanding the evolution of dust properties. A major observational contributor to this field is the investigation of dust properties deduced from dust infrared (IR) excess in the spectral energy distribution (SED; e.g. see various recent results from *Spitzer* surveys, such as Sargent et al. 2009; Watson 2009; Juhász et al. 2010; McClure et al. 2010; Oliveira et al. 2010; Manoj et al. 2011; Oliveira et al. 2011, etc., and references therein). However, the exact details of the spatial disc structure are difficult to determine from the SEDs alone, because of the intrinsic mathematical degeneracy of models that reproduce only flux measurements (Vinković et al. 2003). This makes the direct imaging of protoplanetary discs an indispensable tool in the exploration of their properties, but it also poses difficult challenges for theoretical models (e.g. Millan-Gabet et al 2007; Watson et al. 2007; Dullemond & Monnier 2010; Williams & Cieza 2011).

The innermost disc regions, within a few astronomical units (au) around the central star, have attracted special attention in this field

★E-mail: vinkovic@pmfst.hr

of research, because the formation of terrestrial-type planets is expected in this disc zone. It is also a zone of dust sublimation, high gas densities and complex dust dynamics (e.g. Ciesla 2009; Vinković 2009; Hughes & Armitage 2010; Turner, Carballido & Sano 2010; Armitage 2011). At the same time, it is a very difficult observational target because of its small scale and its proximity to the central star (Millan-Gabet et al 2007). The development of semi-analytical models, inspired by the observed properties of the near-infrared (NIR) part of SEDs, was a strong incentive for the theoretical exploration of inner disc regions (Dullemond & Monnier 2010). This is the part of the spectrum where the inner disc emits, because of its most resilient dust grains, which survive up to temperatures of 1500–2000 K.

In recent years, there has been a tendency to improve upon the existing models. One motivation for this comes from observations that show various features, which cannot be accommodated by the existing simplified and time-steady models (Dullemond & Monnier 2010). Another motivation for the improvements comes from theoretical investigations into the radiative transfer, grain and gas composition and disc geometry of the inner disc. Some examples of these investigations are the following:

(i) the truncation of the inner disc by dust sublimation results in a curvature of the inner disc's rim (Isella & Natta 2005; Tannirkulam, Harries & Monnier 2007);

(ii) multigrain dust models result in complicated geometries and density distributions (Kama, Min & Dominik 2009);

(iii) large grains are grey in the NIR, experiencing maximum temperature within the dust cloud and not at the very surface exposed to the starlight (Vinković 2006; Kama et al. 2009);

(iv) dust dynamics is influenced by radiative pressure and magnetic fields in complicated ways (Vinković 2009; Turner et al. 2010);

(v) dust and gas are thermally decoupled in optically thin regions, which makes gas hotter than initially expected (Thi, Woitke & Kamp 2011);

(vi) gas itself can be a significant source of NIR flux and/or optically thin dust survives closer to the star than the optically thick inner disc's rim (Tannirkulam et al. 2008; Benisty et al. 2010).

In this series of papers, we investigate various theoretical and numerical improvements in the modelling of the inner disc's structure. We start with a study of the improved numerical reconstruction of the dust's thermal structure under the condition of multigrain dust composition. We use passively heated discs as a necessary initial step in identifying the most basic radiative transfer effects. Our focus is on the coexistence of small and large dust grains, because these two dust properties yield large differences in dust sublimation behaviour. When used alone, small grains sublimate at considerably larger distances from the star than large grains. However, when mixed together, they can coexist at distances dictated by the large grains; however, quantitative details are not yet known. Another problem arises from the complicated behaviour of the temperature of the large grains under direct exposure to stellar heating. As mentioned above, the temperature initially increases with optical depth, reaches its maximum at some optical depth, and then decreases as we move deeper into the optically thick interior of the disc. Because dust sublimation is typically used as a unique boundary condition for the structure of the inner disc, we explore how reliable this assumption is in a high-resolution numerical reconstruction of the multigrain dust temperature. In Section 2, we describe some caveats in the numerical treatment of the problem. In Section 3, we describe the obtained temperature structure and the disc images and spectra. We discuss the implications of our findings in Section 4.

2 RADIATIVE TRANSFER MODELLING

2.1 Description of the model

The main focus of this work is on the high-resolution radiative transfer and analysis of the surface of a dusty disc. Hence, we simplify the problem of vertical disc structure and use the model developed by Shakura & Sunyaev (1973). The gas and dust are well mixed and the number density of dust particles of type α in the cylindrical coordinate system (ϱ, z) is

$$n_\alpha(\varrho, z) = N_\alpha \varrho^{-p} \exp\left(-h_0 \frac{z^2}{\varrho^{2m}}\right), \quad (1)$$

with parameters $p = 2$, $m = 1.25$ and $h_0 = 1800$. The coordinates (ϱ, z) used in our calculations are scaled with the smallest distance of dust from the star. We call this the inner disc radius $R_{\rm in}$, and it is located in the mid-plane of the disc. This distance is not known in advance and is a part of the output from the radiative transfer calculation. The outer disc radius is fixed to $R_{\rm out} = 100\,R_{\rm in}$. The number density of the dust grains α at $\varrho = 1$ and $z = 0$, which is the location of radius $R_{\rm in}$, is equal to $N_\alpha = n_\alpha(1, 0)$. We use olivine dust opacities from Dorschner et al. (1995) and two coexisting grain types α with radii of 0.1 and 2 μm. The cross-sections of these are shown in Fig. 1. The ratio of their number densities at (1, 0) is fixed to $N_{0.1}$: $N_2 = 10^4$: 1. The dust sublimation temperature is $T_{\rm sub} = 1500$ K. The spectral shape of the stellar radiation is taken from the Kurucz (1994) model atmosphere for a star with $T_* = 10\,000$ K.

Instead of fixing the absolute value of dust densities, our radiative transfer calculation works with a fixed optical depth along an arbitrary radial line. We use the visual optical depth $\tau_{\rm V} = 10^4$ at 0.55 μm toward the star in the mid-plane of the disc. This optical depth is a line integral of dust visual cross-sections ($\sigma_{0.1,\rm V}$ and $\sigma_{2,\rm V}$) and dust number densities ($n_{0.1}$ and n_2). However, we do not know the integral limits in advance because our two dust types sublimate at different distances from the star. We expect the 2-μm grains to survive closer to the star than the 0.1-μm grains because they are better emitters in the NIR (see Fig. 1), where $T_{\rm sub}$ has its spectral maximum. This means that the 2-μm grains are cooled more efficiently and exist at $R_{\rm in}$, while the sublimation front for the 0.1-μm grains is not known in advance.

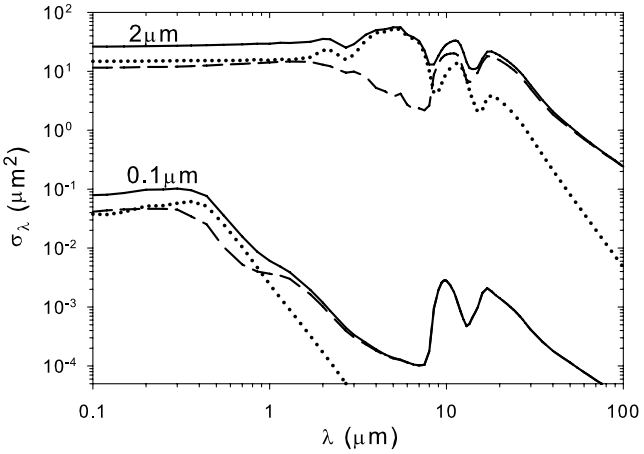

Figure 1. Cross-section of olivine dust grains (Dorschner et al. 1995) used in modelling with radii of 0.1 and 2 μm. The dashed, dotted and solid lines represent emission, scattering and total extinction cross-section, respectively.

In the end, we see that in our optically thick example the smaller grains survive very close to $R_{\rm in}$ because the larger grains shield them from direct stellar radiation. This simplifies the optical depth integral

$$\tau_{\rm V} = \int_{\approx 1}^{R_{\rm out}/R_{\rm in}} \left[\sigma_{0.1,{\rm V}} n_{0.1}(\varrho, 0) + \sigma_{2,{\rm V}} n_2(\varrho, 0)\right] R_{\rm in}\, {\rm d}\varrho. \quad (2)$$

Using equation (1), we can derive the dust density scale as

$$N_{0.1} = \frac{\tau_{\rm V}}{\left(\sigma_{0.1,{\rm V}} + \sigma_{2,{\rm V}} N_{0.1}/N_2\right)(1 - R_{\rm in}/R_{\rm out})\, R_{\rm in}}. \quad (3)$$

This equation shows that the density scale is directly related to the distance scale $R_{\rm in}$. Using the values for our parameters in equation (3) gives

$$N_{0.1} = \frac{3.76 \times 10^8}{(R_{\rm in}/{\rm R}_\odot)} {\rm m}^{-3}.$$

Because we do not know $R_{\rm in}$ in advance, we also do not know the absolute density scale.

To solve the radiative transfer problem, we only need to specify $T_{\rm sub}$ and T_*, the optical depth $\tau_{\rm V}$, the spectral shape of the dust cross-sections and the shape of the stellar spectrum. All other properties can be expressed in dimensionless terms. This is a consequence of the intrinsic degeneracy of radiative transfer equations, as shown by Ivezić & Elitzur (1997) in their derivation of the general scaling properties of the radiative transfer problem for radiatively heated dust. Luminosity L_* is irrelevant and it enters as a parameter only after we obtain $R_{\rm in}$ in units of stellar radii R_* from the output of the radiative transfer calculation. Then, we can scale our model according to the stellar radius derived from the luminosity:

$$R_* = {\rm R}_\odot \left(\frac{{\rm T}_\odot}{T_*}\right)^2 \left(\frac{L_*}{{\rm L}_\odot}\right)^{0.5}.$$

2.2 Boundary condition at the inner rim

$T_{\rm sub}$ is the parameter that has been traditionally used as a boundary condition for the inner rim of dusty discs. The physical motivation for this was the expectation that the dust temperature of externally heated dusty clouds always monotonically decreases with the increasing distance from the heat source. This means that the maximum dust temperature is achieved at the closest distance to the star that a dust particle can reach before sublimating away.

However, this concept was found to be incorrect in the case of externally heated optically thick clouds made of large ($\gtrsim 1$ μm) dust grains. Such grains have an ability to efficiently absorb the diffuse IR radiation originating from the clouds interior. This results in an increase of the temperature within the dust cloud at the visual optical depth of $\tau_{\rm V} \sim 1$, rather than on the very surface exposed to the stellar heating. This process of temperature inversion is similar to the greenhouse effect. It was first discovered numerically in single-grain-size models (Dullemond 2002; Isella & Natta 2005; Vinković et al. 2006) and then proved analytically for multigrain dust mixtures (Vinković 2006). The analytical analysis has shown that large grains dominate the cloud's surface, while smaller grains can exist immediately behind the zone of temperature inversion. The analysis has also shown that the effect exists for both types of radiative transfer boundary conditions: (i) a constant external flux heating the cloud, with no limits on the dust temperature; (ii) a fixed maximum dust temperature, corresponding to dust sublimation.

The inner regions of protoplanetary discs provide ideal conditions for the emergence of the temperature inversion phenomenon. Accretion, which is ubiquitous to protoplanetary discs, constantly resupplies the inner regions with large grains that grow in the disc. Hence, optically thick discs should be in a permanent process of minimization of their inner disc radius, with large grains populating the inner disc's surface and dictating the radiative transfer. A complication arises when we try to deal with the spatial scale of the disc's surface because the surface is defined by the optical depth of $\tau_{\rm V} \lesssim 1$ as a zone where most of the stellar radiation is absorbed. Therefore, this optically thin zone is not necessarily geometrically thin. Instead, it could extend much closer to the star, creating a large optically thin dusty zone that spreads over radii smaller than the inner radius of the optically thick disc. Because dust can exist only up to its sublimation temperature, Vinković (2006) proposed using two inner radii that discriminate between these two coexisting, optically thin and thick, disc zones:

$$R_{\rm in} = \frac{\Psi R_*}{2} \left(\frac{T_*}{T_{\rm sub}}\right)^2. \quad (4)$$

Here, $\Psi = 2$ and $\Psi \sim 1.2$ are used for the optically thick (Dullemond, Dominik & Natta 2001) and optically thin (Vinković et al. 2006) inner radii, respectively. Note that, here, we assume that the disc opacity is dominated by large grains that have grey opacity in the NIR. Smaller grains are inefficient emitters of NIR radiation and therefore they overheat and sublimate away at these distances from the star. Smaller grains can survive either at larger distances from the star or hidden in the disc's interior behind grey dust.

Kama et al. (2009) have shown these effects numerically, using discs with various dust compositions and surface densities. The optically thick radius in their models, dominated by large grains, is in agreement[1] with equation (4). The optically thin zones in their models are dictated by predefined power-law density profiles and therefore do not extend to the theoretical minimum distance to the star.

The models of Kama et al. (2009) demonstrate the boundary-condition problem that we face when the spatial dust density distribution of the optically thin zone is free to vary. In order to simplify the problem and to make it manageable, in this paper we do not explore the properties of the optically thin zone. Our goal is limited to the exploration of the temperature inversion structure in two dimensions and to the survival of small grains in the disc. We achieve this by fixing the maximum dust temperature anywhere in the disc to $T_{\rm sub}$. This means that we do not know the dust temperature $T_{\rm in}$ at $(\varrho = 1, z = 0)$, but we expect it to be smaller than $T_{\rm sub}$.

Such a boundary condition is easy to postulate, but it creates substantial numerical challenges, especially in the case of a high-resolution temperature calculation like ours. Our numerical approach was semi-autonomous, where the computational grid updates and $T_{\rm in}$ corrections were checked by hand for precision and error control. We know in advance that the 2-μm grains in our model should survive at all grid points. However, the 0.1-μm grains must be removed from the surface of the inner disc where these grains overheat. They survive only in the interior shielded by the 2-μm grains, but the exact location of their survival is not known in advance.

We look for a solution by iterating between radiative transfer calculations and dust removal. These iterations were combined by making corrections of $T_{\rm in}$ by hand. In addition, we updated the

[1] Small deviations from equation (4) are visible in their models because they use the dependence of dust sublimation on gas density, which slightly increases the dust sublimation temperature at the rim of the inner disc.

computational grid structure after each dust removal, because our grid is irregular and automatically traces spatial and optical depth gradients. Even though most of this iterative process is automatic, we had to check each step by hand to avoid errors and grid imperfections. None the less, small deviations from $T_{\rm sub}$ are very difficult to suppress, but we managed to keep the error within 3 per cent (45 K for $T_{\rm sub} = 1500$ K).

2.3 Radiative transfer calculation

Numerical radiative transfer calculations were performed using the code LELUYA (http://www.leluya.org). This solves the integral equation of the formal solution of radiative transfer with axially symmetric dust configurations, including dust scattering, absorption and thermal emission. The solution is based on a long-characteristics approach to the direct method of solving the matrix version of the integral equation (Kurucz 1969). The equations are solved on a highly unstructured triangular self-adaptive grid, which traces simultaneously both the density gradients and the optical depth gradients over many orders of magnitude in spatial and optical depth space. The code is parallelized and written in C. Theoretical and computational details are explained by Vinković (2003).

The key for a high-resolution temperature structure is the grid used in our calculations. The code creates a grid by integrating optical depth along lines that cut through the largest optical depth gradients. In our case, these are radial lines and vertical lines parallel to the symmetry axis. The grid vertices are chosen on these lines according to

$$\frac{\triangle\tau}{\tau} + \frac{\triangle L}{L} = 2, \qquad (5)$$

where $\triangle\tau$ and $\triangle L$ are the optical-depth and spatial steps, respectively (both are calculated relative to the last created grid vertex) and τ and L are the optical depth and the spatial distance from the starting point of integration, respectively. If used carefully, with starting points in low-density areas and at dust sublimation surfaces, this equation enforces higher grid resolution in zones of optical depth gradients. Vertices in the optically deep interior are distributed more sparsely because the radiation field is slowly varying. In addition to the generation of this automatic grid, we also inspected the grid by eye and added extra grid vertices where we considered it necessary. The final grid is shown in Fig. 2.

Each grid vertex contains an angular grid that defines the directions of integration of the radiative transfer equation. It would be simple and fast to always use the same type of angular grid, but vertices on the disc surface are surrounded by an anisotropic radiation field, which changes its geometry from vertex to vertex. Therefore, we use a method where a unit sphere is split self-adaptively into small spherical triangles according to the number of vertices visible through a triangle in three-dimensional space. This enables increased resolution in the directions of radiation field gradients. The surfaces of spherical triangles are used as corresponding statistical weights in the discretized angular integration.

3 RESULTS

We obtained the inner disc radius of $R_{\rm in} = 44.72R_*$, which agrees with equation (4) for the case of an optically thick edge of a dusty disc. In real units, this corresponds to $R_{\rm in} = 0.0687(L_*/{\rm L}_\odot)^{0.5}$ au for a 10 000-K star. Typical luminosities of Herbig Ae stars are $L_* = 20$–$100\ {\rm L}_\odot$, so typical values for the inner optically thick radius of a disc are $R_{\rm in} = 0.31$–0.69 au.

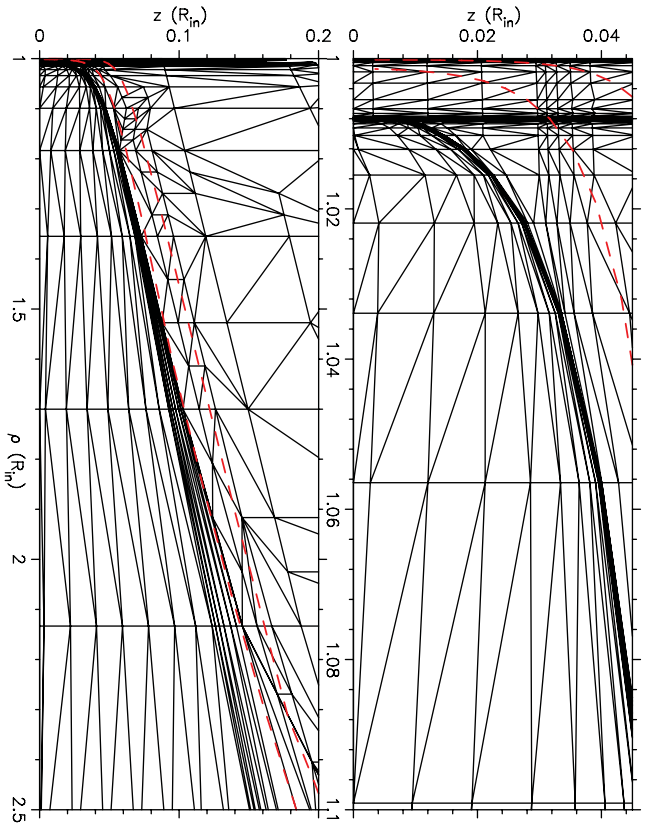

Figure 2. Computational grid used in the final model. The panels show two spatial scales of the inner disc region in cylindrical coordinates (ϱ, z). Thick dashed lines are radial visual optical depths of $\tau_{\rm V} = 0.1$ and $\tau_{\rm V} = 1$. A section of the grid with increased resolution traces the surface of the disc populated with 0.1-μm grains, while 2-μm grains exist at all grid vertices.

3.1 Temperature structure

The dust-temperature distribution is shown in Fig. 3 for both 2- and 0.1-μm grains. The optically thin surface of the disc is populated only by large grains at distances $\varrho \lesssim 2.2$ from the star. However, smaller grains survive in the optically thick interior of the disc, where they are heated by diffuse IR radiation and protected from direct stellar radiation. This enables smaller grains to survive almost as close as $R_{\rm in}$ to the star.

The temperature inversion effect is reproduced by our model, with the temperature maximum at $\tau_{\rm V} \sim 1.5$ in the optical depth space and at $\sim$1.005 $R_{\rm in}$ from the star. As a result of this effect, the temperature decreases very slowly with the optical depth and the zone of high dust temperature is not confined to a geometrically thin disc edge. By high temperature, we mean temperatures high enough to quickly anneal the silicates (Hill et al. 2001), which is $\gtrsim$ 950 K. In Fig. 3, we can see that the disc temperature is above 950 K between $R_{\rm in}$ and $\sim$1.1 $R_{\rm in}$, which is geometrically a significant part of the inner disc.

A more detailed insight into the temperature structure is given in Figs 4 and 5. These figures show cuts through the disc along radial lines of different angles θ relative to the symmetry axis (z-axis). Fig. 4 displays the dust temperature relative to the radial optical depth. In the mid-plane ($\theta = 90^\circ$), the temperature remains above the annealing limit of 950 K almost until $\tau_{\rm V} \sim 10^3$. Small grains sublimate at $\tau_{\rm V} \sim 4$–6 and their temperature drops faster than the temperature of larger grains, such that both grain

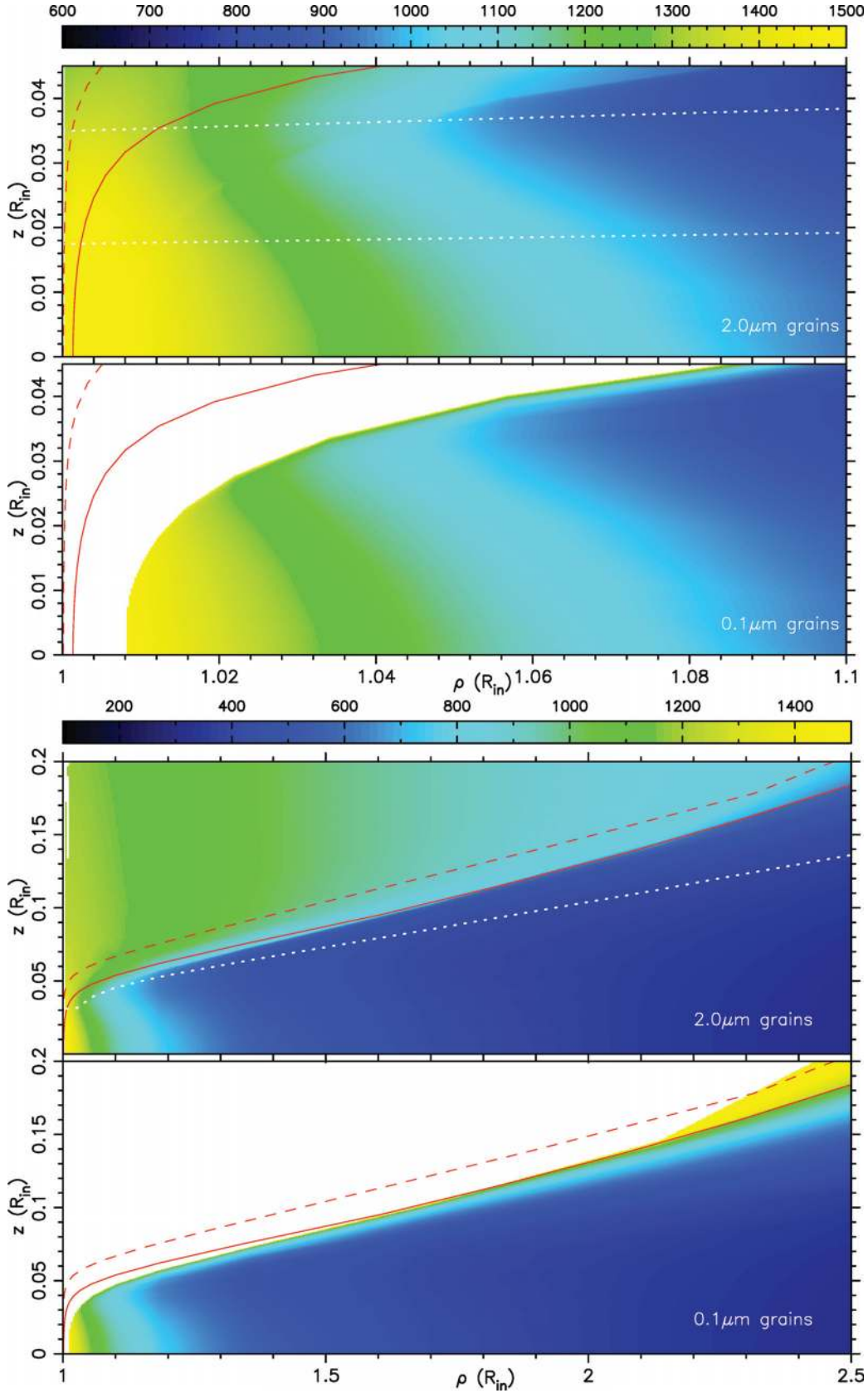

Figure 3. Temperature of dust grains shown at two spatial scales in cylindrical coordinates for two coexisting grain radii (indicated in the images). The dashed line indicates the radial optical depth of $\tau_V = 0.1$, while the solid line is $\tau_V = 1$. Note how 0.1-μm grains survive in the optically thin disc surface only at radial distances of $\varrho \gtrsim 2.2$, but in the disc's interior they exist very close to R_{in}. The dotted lines in the top panel indicate the radial lines of the 88° and 89° inclination angles used in Figs 4 and 5. The dotted line in the third panel from the top shows the vertical optical depth of $\tau_V = 1$.

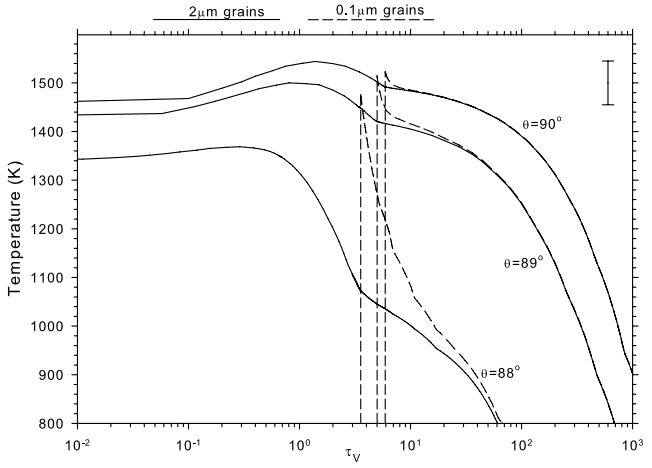

Figure 4. Temperature profiles along radial visual optical depth lines for different inclination angles θ relative to the symmetry axis (z-axis): 90° (mid-plane), 89° and 88° (shown in Fig. 3 as dotted lines in the top panel). The solid and dashed lines indicate the temperature of 2- and 0.1-μm grains, respectively. The error bar marks the 3 per cent error tolerance on the dust sublimation temperature of 1500 K.

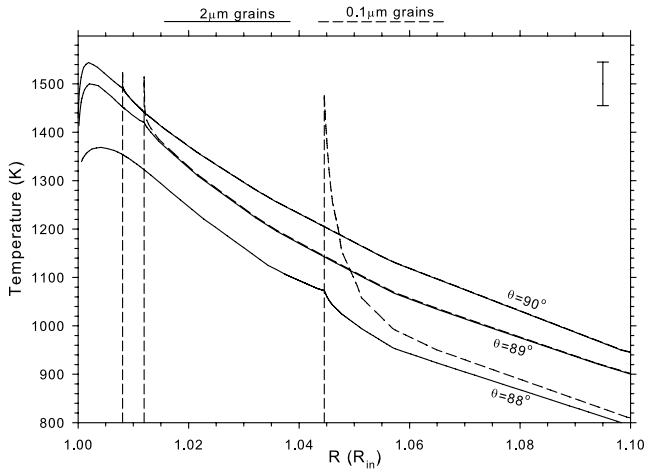

Figure 5. Same as Fig. 4, except that the temperature is shown relative to the spatial scale $R = (\varrho^2 + z^2)^{0.5}$ along the radial lines. The steep decline in temperature for 0.1-μm grains explains the increased grid resolution in the sublimation zone of 0.1-μm grains (see Fig. 2).

sizes reach the same temperature at $\tau \gtrsim 10$. This is in agreement with the qualitative theoretical predictions by Vinković (2006). The cut along $\theta = 88°$ shows a slower decline for the temperature of 0.1-μm grains, because this cut goes through the disc region where the largest temperature gradient is perpendicular to the disc plane (see the upper dotted line in the top panel in Fig. 3).

Fig. 5 displays the same radial cuts as in Fig. 4, but relative to the spatial distance from the star. Here, we can see that the dust temperature in the mid-plane remains above 950 K almost up to $1.1\,R_{\rm in}$. Small grains sublimate at distances from $1.008\,R_{\rm in}$ (mid-plane) to $1.045\,R_{\rm in}$ (for $\theta = 88°$). The temperature gradient for 0.1-μm grains is very steep between the point of $T_{\rm sub}$ and the point of thermalization with 2-μm grains. This explains why the computational grid has such a high resolution in the region of 0.1-μm dust sublimation (see Fig. 2). The spatial step in this region goes as low as $\triangle L = 3.7 \times 10^{-6}\,R_{\rm in}$.

The temperature of the 2-μm grains is slightly increased at the sublimation location of 0.1-μm grains. The effect is small because the NIR emissivity of the 0.1-μm grains is too small to provide a significant contribution to the local diffuse radiation. This would not be the case if the number density of larger grains were reduced to levels where the diffuse radiation is dominated by smaller grains. However, this would also mean that larger grains do not dominate the optical depth and, in turn, cannot shield smaller grains. This would result in a larger inner disc radius dictated by the opacity of smaller grains.

Another way of observing the disc temperature structure is to focus on how deep we can see into the disc. For example, the dotted line in the third panel from the top in Fig. 3 shows the optical depth of $\tau_{\rm V} = 1$ when the disc is viewed face on. This is approximately the depth of the observable disc at a wavelength of 0.55 μm. Fig. 6 shows the dust-temperature distribution at the optical depth of $\tau = 1$ at a wavelength of 2.2 μm for different inclination angles. This reveals that we can see deep enough into the disc to sample both dust types, even in the regions where smaller grains do not populate the disc surface.

3.2 Spectra and images

The SED of protoplanetary discs traces the dust emission and scattering at different temperatures and optical depths. The inner disc region experiences the highest temperatures and it should be detectable at NIR and mid-IR wavelengths. Large optical depths prevent the photons of these wavelengths from the deep disc interior from being detected; hence, the optically thin disc surface dominates the flux. Fig. 7 shows SEDs of the model viewed face-on (inclination angle $\theta = 0°$) and inclined ($\theta = 45°$ and $\theta = 70°$). The SEDs do not differ at short wavelengths where the stellar flux dominates. They also do not differ at the far-IR wavelengths where the disc becomes optically thin to its own emission.

The relative contribution of stellar flux, dust emission and scattering to the total SED is shown in Fig. 8 for a 45° disc inclination. Inclination decreases the scattering contribution and increases the contribution of dust emission, but the overall wavelength variation is similar to this face-on example. The competition between dust emission and scattering for dominance in the IR part of the spectrum (see Fig. 9) is closely matched with their interplay in the dust opacity shown in Fig. 1. The dominance of large grains in the disc surface leads to a strong contribution of dust scattering in the near- and mid-IR. The details depend on the chosen dust properties, but the overall trend indicates that scattering is a significant contributor to the SED.

The near- and mid-IR parts of the SED decrease approximately as $\cos\theta$ for small or intermediate angles. The surface is geometrically thin and $\cos\theta$ comes from the geometrical projection of the emitting surface. For larger inclination angles, the SED decreases more slowly than $\cos\theta$, because the line of view is grazing the disc surface and its geometrical thickness is no longer negligible. A different SED behaviour is visible at 2–3 μm where the flux is almost independent of inclination for small angles, and then decreases only slightly with larger angles. These are wavelengths where the inner disc edge emits at a temperature of $T_{\rm sub}$. The curvature and vertical height of the inner disc edge enable its emission to be almost insensitive to θ, until the inclination becomes large (Isella, Testi & Natta 2006; Tannirkulam et al. 2007; Thi et al. 2011).

The model images shown in Fig. 10 demonstrate this. The inner disc edge is the brightest feature in the 2.2-μm images and inclination exposes its curvature. At 10 μm, the disc edge is not

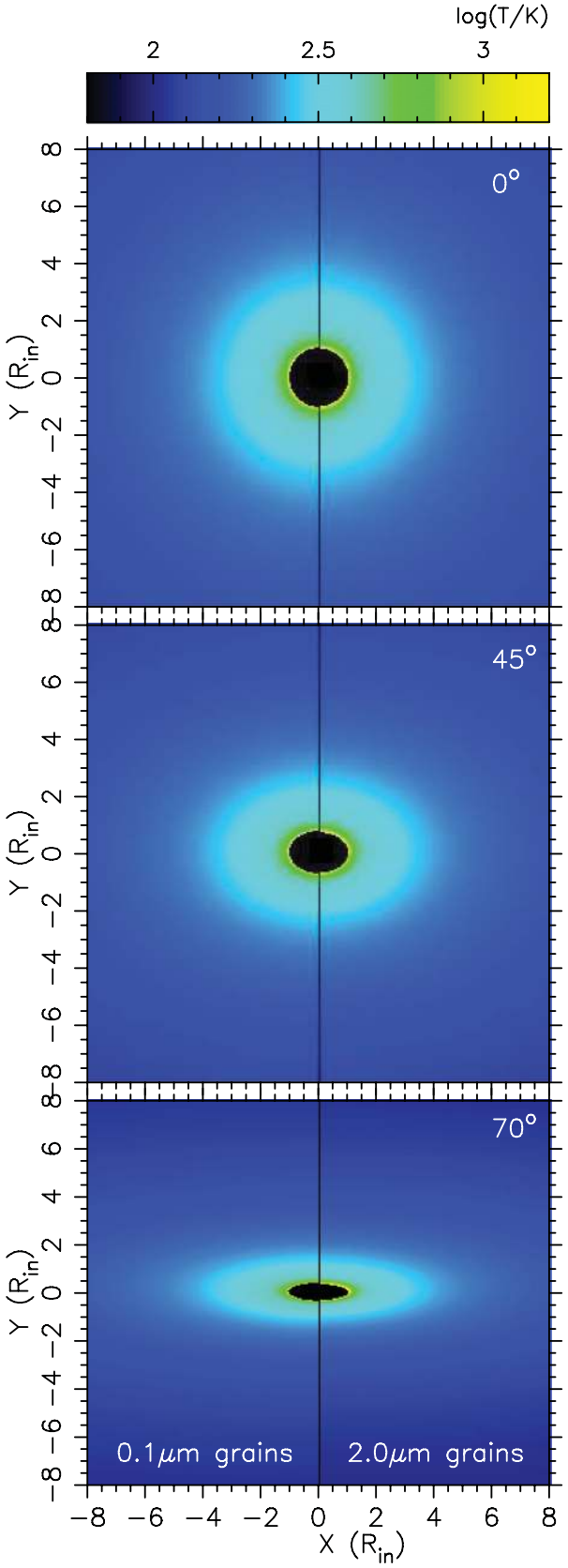

Figure 6. Map of temperature along the line of sight for different inclination angles. The images show temperatures at optical depth $\tau = 1$ for the 2.2-μm wavelength. The left and right sides of the images show temperatures for 0.1- and 2-μm dust grains, respectively.

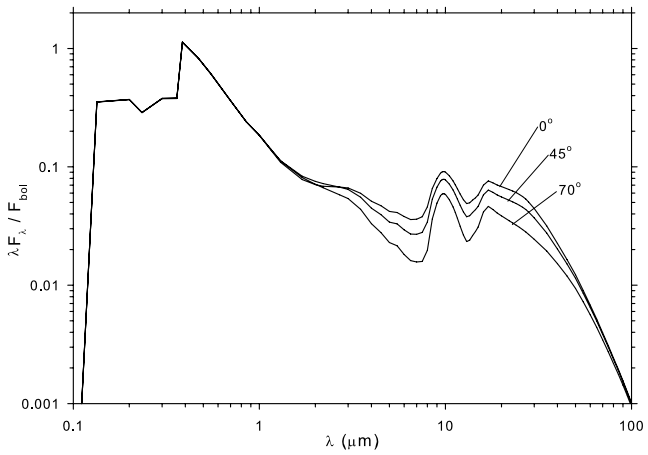

Figure 7. SED of the model for three different disc inclination angles: 0° (face-on), 45° and 70°.

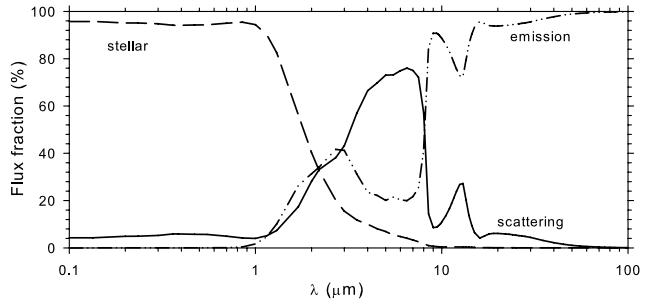

Figure 8. Wavelength variation of the relative contribution of stellar, emission and scattering flux to the total flux for a 45° disc inclination. Other inclinations have very similar relative contributions. Note the dominance of scattering in the NIR as a result of large 2-μm grains (see also the dust cross-sections in Fig. 1).

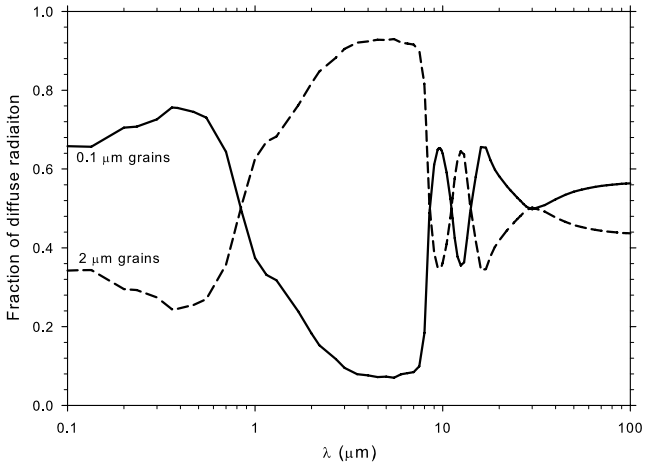

Figure 9. Wavelength variation of the relative contribution of 0.1- and 2-μm grains to the total observed diffuse flux for a 45° disc inclination. Other inclinations have very similar relative contributions. Note how the 2-μm grains dominate the NIR because the opacity of the 0.1-μm grains drops quickly in this wavelength region (see Fig. 1).

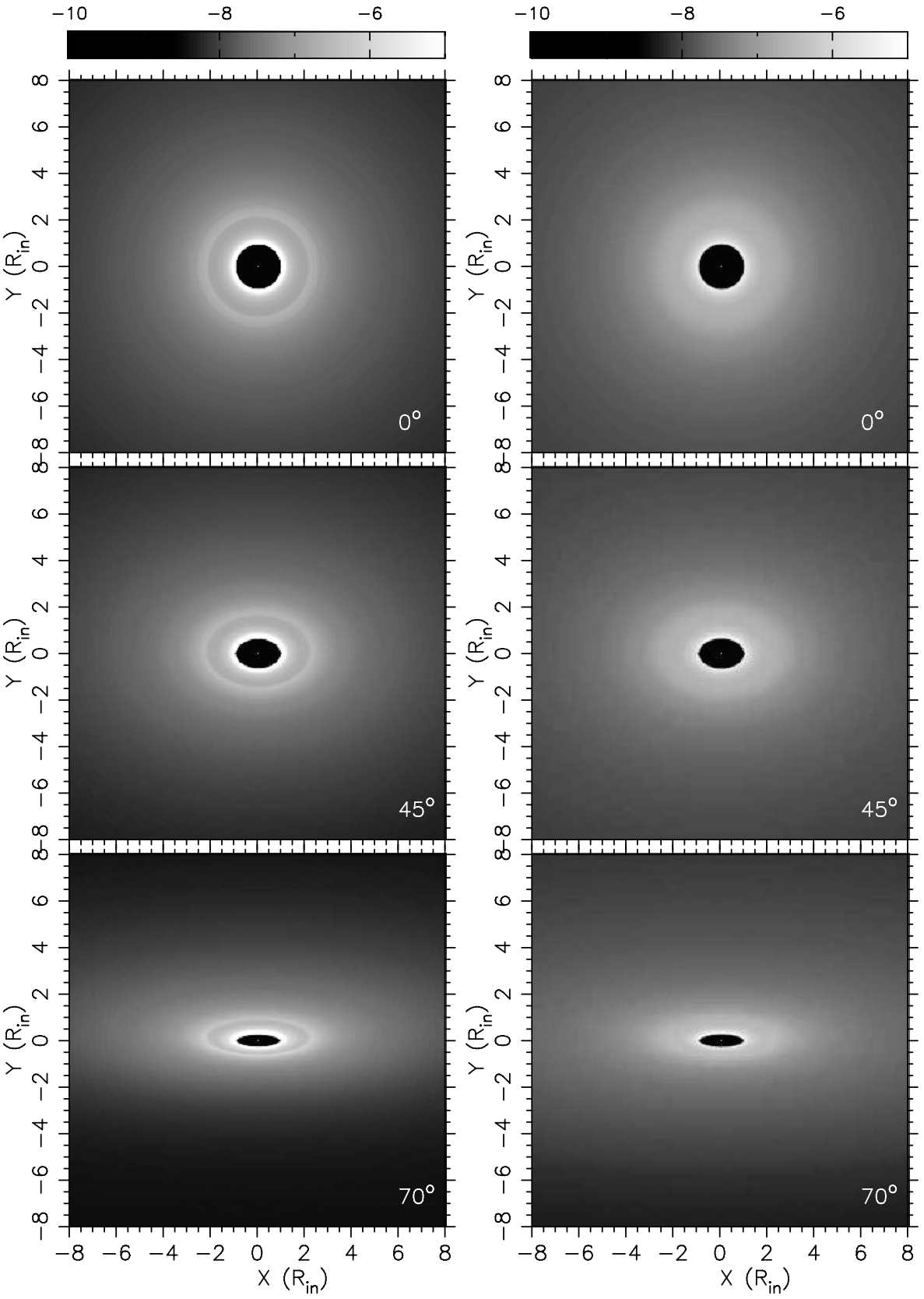

Figure 10. Model images at wavelengths of 2.2 μm (left column) and 10 μm (right column) for different inclination angles. Images at wavelengths $\lesssim 8$ μm show brightness behaviour similar to this example. A faint brightness ring in images at $\sim 2R_{\rm in}$ distance from the centre is a feature caused by 0.1-μm grains on the disc's surface. The flux through each image pixel is scaled with the bolometric flux $F_{\rm bol}$. Contributions from 0.1- and 2-μm dust grains to the model images are shown in Fig. 11.

the main feature and the rest of the disc surface dictates the SED. Disentangled contribution from both grains sizes to the disc images is shown in Fig. 11. The brightness of the inner disc edge is dominated by large grains, but smaller grains also contribute, despite being positioned optically deeper within the disc. A faint ring visible at a distance of ∼2.2 from the image centre is the location where smaller grains show up in the disc surface.

The NIR images and SED are obviously highly sensitive to the curvature of the inner disc edge. This is why its height and shape have been of great interest to astronomers (Millan-Gabet et al 2007; Dullemond & Monnier 2010). However, the rest of the disc surface also contributes to the image flux. In Fig. 12, we show how dust scattering and emission differ in their contribution to the disc surface brightness at wavelengths of 2.2 and 10 μm. The thermal emission is modulated by the dust emissivity and reddened by dust layers along the line of sight. Fig. 6 shows the temperature distribution across the 2.2-μm image at a $\tau = 1$ optical depth, which approximately shows how deep we see into the disc. From Fig. 12, we can see that temperatures of the 2-μm grains, which contribute most to the thermal emission at NIR wavelengths, are limited to small radii close to the inner disc edge, while 0.1-μm grains contribute over a larger area, but with smaller surface brightness because of their smaller emissivity. In the mid-IR, both grains have thermal emission spread over a larger area. Because the 0.1-μm grains appear on the disc's surface layer at $\varrho \sim 2.2$, we can see an increase in brightness for the images at this distance from the centre. However, this increase is small because the emissivity of the 0.1-μm grains is small compared to 2-μm grains. This is why large grains dominate the SED and images in the NIR, even though smaller grains have high temperatures over a larger portion of the disc's surface.

While the emission is confined to small radii where the dust is hottest, scattering follows surface dust density and extends further away. Pinte et al. (2008) have shown how scattering is an important component in the interpretation of the NIR imaging data. We need to emphasize here that our images are calculated with an isotropic scattering function, which is a rough approximation for large grains. A more realistic scattering function would yield larger image asymmetries with inclination.

4 DISCUSSION AND CONCLUSIONS

In this paper, we have explored the temperature structure of the hottest dusty regions of protoplanetary discs. Here, in the most inner part of the disc, the interplay of dust density, optical depth and multigrain dust composition creates an intricate disc-surface structure shaped by non-uniform sublimation of individual dust species. Our study was limited to two distinctively different dust grain radii of 0.1 μm (small) and 2 μm (large). These grains exhibit very different sublimation behaviours when used individually in single-grain models, with large grains surviving much closer to the star than small grains. However, we have demonstrated a significant decrease in the sublimation distance of small grains when they are mixed with large grains when large grains dominate the opacity. Small grains survive behind the visual optical depth of $\tau_V \sim 4$–6 for the large grains, which translates into a sublimation distance only a few percentage points larger than that for large grains. We argue that the disc accretion constantly resupplies the inner disc with large grains, which enables these to dominate the opacity and to sustain the conditions described in our paper. There are also observational confirmations of this inner disc property; the spectra indicate large fractions of large grains on the surface of inner discs (e.g. van Boekel et al. 2004, 2005; Sargent et al. 2009; Watson 2009; Juhász et al. 2010), while the observed sizes of inner discs are consistent with large grains dictating the inner disc radius R_{in} (Millan-Gabet et al 2007).

Our study required a very high self-adaptive computational grid resolution (almost $10^{-6} R_{in}$) in order to correctly trace dust sublimation and temperature gradients. Computations have to resolve two important temperature gradients. One is the temperature inversion experienced by large grains, where the temperature reaches its maximum at $\tau_V \sim 1.5$ instead of the very surface exposed to the stellar radiation. The other comes from the tendency of small grains to quickly thermalize with large grains as the optical depth increases, which results in a steep temperature decline for small grains. Prior similar studies have not resolved these effects in multigrain dust models (Tannirkulam et al. 2007; Kama et al. 2009), and this signifies the importance of high-resolution radiative transfer calculations.

So far, the implications of the temperature inversion effect, where the dust temperature at R_{in} is lower than sublimation, have received modest attention in the literature (Vinković 2006; Kama et al. 2009; Dullemond & Monnier 2010). The main consequence of this effect is that large grains can survive closer to the star than the optically thick part of the disc. For theorists, this implies that the dusty disc models currently used are incomplete, while the development of a more realistic model will require a scrutiny of the dust dynamics coupled with radiative transfer. For observers, this implies that the optically thin dust might be detectable within the currently used optically thick inner disc radius. The recent detection of disc brightness within R_{in} could be the first indication that such a dust structure exists, but it has to be disentangled from possible gas emission (Tannirkulam et al. 2008; Benisty et al. 2010).

We have also resorted to a simplified boundary condition where the dust density drops to zero at R_{in}, simply because we currently do not have any theoretical understanding of the density structure of optically thin dust within R_{in}. Its structure can be greatly influenced by dust dynamics because of forces other than gravity and gas drag. The force of radiation pressure would act upon all dust grains in this optically thin disc zone. Magnetic fields at these distances could be strong enough to interact with charged dust particles. Charging is expected because of high gas temperatures and exposure to ultraviolet and X-ray radiation (Turner et al. 2010; Pedersen & Ines Gómez de Castro 2011). This leads to the coupling of grain settling to the distribution of the magnetorotational turbulence (Turner et al. 2010). High gas densities also provide conditions for photophoresis on large grains, which moves particles outward (Moudens et al. 2011). Moreover, these dynamical processes could vary optical depth within R_{in}, which would immediately influence the optically thick region where the dust at the sublimation zone can overheat and sublimate. Because this sublimation zone is located within a disc, we do not know how changes in optical depth, caused by dust sublimation, would influence the overall disc structure. All these issues make further work on the temperature structure of the inner disc region a very challenging task (Dullemond & Monnier 2010), which will require the computation of individual trajectories of dust grains coupled with radiative transfer. Such models are still under development for studying the outer, dynamically and thermally simpler, disc regions (e.g. Charnoz et al. 2011).

We have also analysed how differences in the distribution of small and large grains influence the disc spectrum and images. Large grains dominate the NIR spectrum and image flux, because small grains cannot survive in the disc surface up to distances $\gtrsim 2.2\, R_{in}$. None the less, small grains contribute significantly to the image

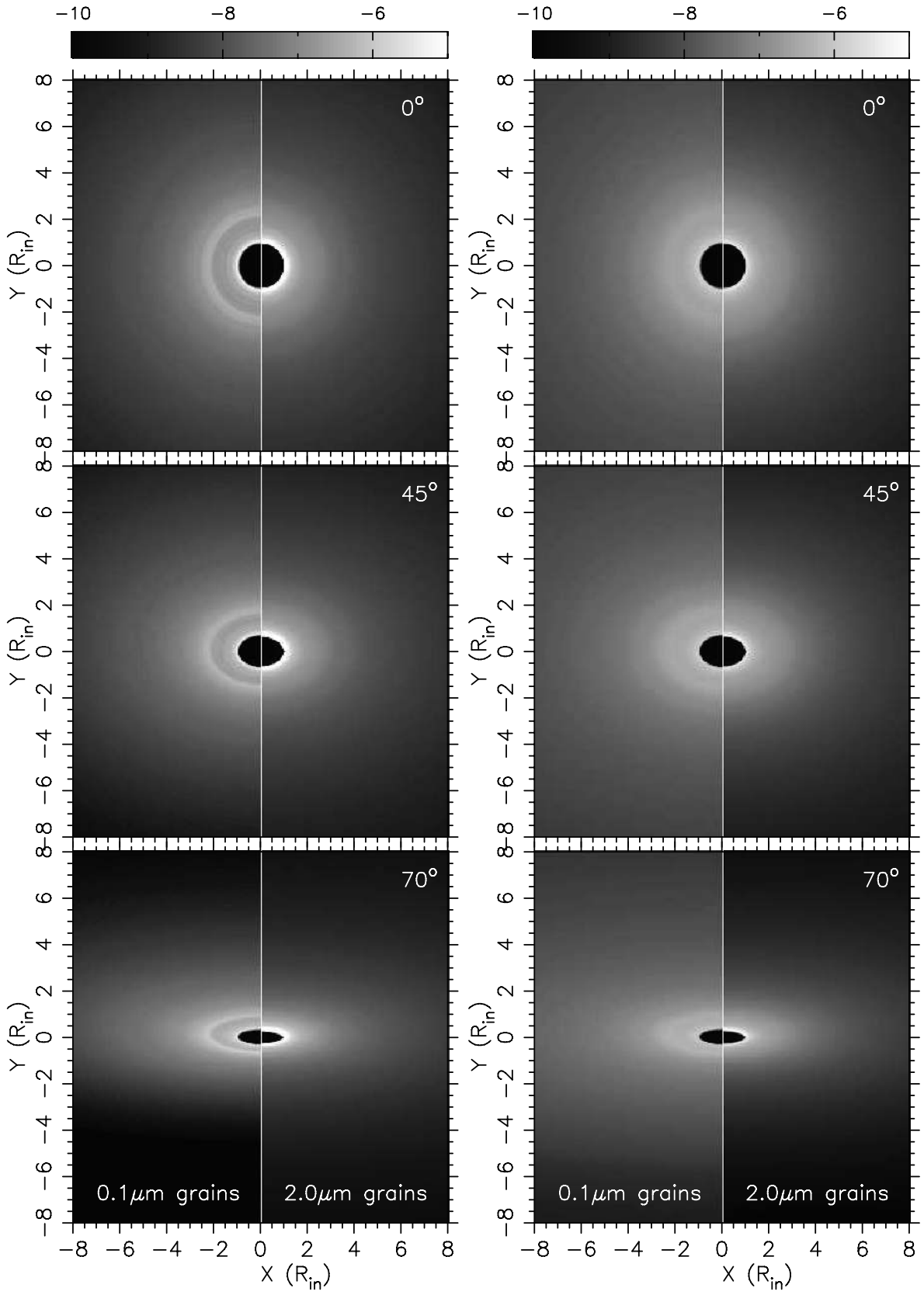

Figure 11. Contributions from 0.1- and 2-μm dust grains to the model images at wavelengths of 2.2 μm (left column) and 10 μm (right column) for different inclination angles. The left and right sides of the images show contributions from 0.1- and 2-μm dust grains, respectively. The flux through each image pixel is scaled with the bolometric flux $F_{\rm bol}$. For the complete images, with both contributions merged, see Fig. 10.

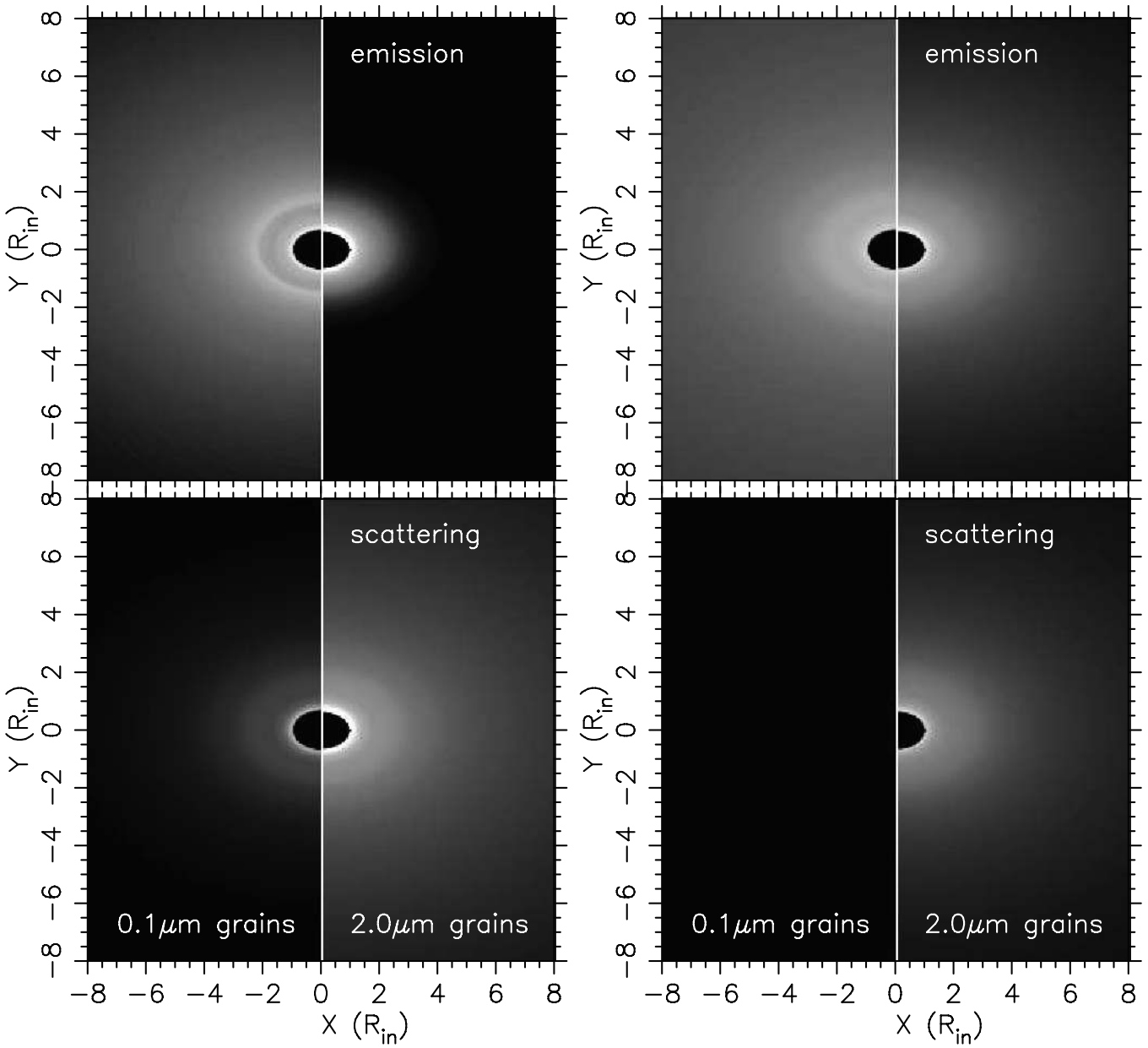

Figure 12. Model image at wavelengths of 2.2 μm (left column) and 10 μm (right column) and a 45° inclination, separated into dust scattering and emission components. The left and right sides of the images show contributions from 0.1- and 2-μm dust grains, respectively. The complete image is shown in Fig. 10.

surface brightness, especially at scales several times larger than $R_{\rm in}$. Hence, when invoking grain growth as an interpretation for a larger fraction of large grains in the inner part of protoplanetary discs, we have to take into account the dominance of large grains in the NIR opacity of the dust mixture and the spatial separation of dust grains by dust sublimation. Notice that, in our model, we use the same ratio of large to small grains throughout the entire disc; nevertheless, their fractional contribution to the SED and images is highly wavelength-dependent.

Dust separation is also caused by the force of radiation pressure, which we will explore in the next paper in this series. Small grains are more easily eroded from the surface of optically thick discs than larger grains because of the radiation pressure from stellar radiation (Takeuchi & Lin 2003). Moreover, Vinković (2009) has shown how large grains experience additional radiation pressure force as a result of the NIR radiation from the hot disc dust, which pulls larger grains out of the disc until the stellar radiation pressure force overcomes the gas drag force and blows grains outward. This process is very fast (within orbital time) unless the local gas density is high enough to dominate over the radiation pressure force. Another important effect is corrections to the vertical size of the inner disc. The inner disc edge is hotter than the standard disc structure, which results in the vertical expansion of the disc (Dullemond et al. 2001; Thi et al. 2011). As long as the disc does not expand so much as to cause self-shadowing, we expect its temperature structure to be qualitatively similar to our model, except for the geometrical scaling of the vertical disc size. Another important thermal effect comes from viscous heating, which increases the temperature in the mid-plane. However, here, we again expect the thermal structure above the mid-plane to be dominated by the effects described in our model,

because this region is dominated by stellar heating (D'Alessio et al. 2006). Overall, the exact dynamical stability of the dusty disc structure, taking into account all these effects, as well as the optically thin dust within $R_{\rm in}$, is still unknown and it requires additional research.

ACKNOWLEDGMENTS

The project described in this paper was performed over many years using various computational facilities. It was supported by the National Computational Science Alliance (NCSA) under AST 04-0006 and utilized the NCSA's Xeon LINUX cluster. The author also thanks the Institute for Advanced Study for time on their LINUX cluster and the University of Zagreb Computing Centre (SRCE) for time on their cluster, Isabella. Finally, the work was completed on the computer cluster, Hybrid, at the Physics Department, University of Split, financed by the National Foundation for Science, Higher Education and Technological Development of the Republic of Croatia.

REFERENCES

Armitage P. J., 2011, ARA&A, 49, 195
Benisty M. et al., 2010, A&A, 511, A74
Charnoz S., Fouchet L., Aleon J., Moreira M., 2011, ApJ, 737, 33
Ciesla F. J., 2009, Icarus, 200, 655
D'Alessio P., Calvet N., Hartmann L., Franco-Hernández R., Servín H., 2006, ApJ, 638, 314
Dorschner J., Begemann B., Henning T., Jaeger C., Mutschke H., 1995, A&A, 300, 503
Dullemond C. P., 2002, A&A, 395, 853
Dullemond C. P., Monnier J. D., 2010, ARA&A, 48, 205
Dullemond C. P., Dominik C, Natta A., 2001, ApJ, 560, 957
Hill H. G. M., Grady C. A., Nuth J. A. III, Hallenbeck S. L., Sitko M. L., 2001, Proc. Nat. Acad. Sci., 98, 2182
Hughes A. L. H., Armitage P. J., 2010, ApJ, 719, 1633
Isella A., Natta A., 2005, A&A, 438, 899
Isella A., Testi L., Natta A., 2006, A&A, 451, 951
Ivezić Ž., Elitzur M., 1997, MNRAS, 287, 799
Juhász et al., 2010, ApJ, 721, 431
Kama M., Min M., Dominik C., 2009, A&A, 506, 1199
Kurucz R. L., 1969, ApJ, 156, 235
Kurucz R. L., 1994, CD-ROM No. 19, Smithsonian Astrophys. Obs.
McClure M. K. et al., 2010, ApJS, 188, 75
Manoj P. et al., 2011, ApJS, 193, 11
Millan-Gabet R., Malbet F., Akeson R., Leinert C., Monnier J., Waters R., 2007, in Reipurth B., Jewitt D., Keil K., eds, Protostars and Planets V. Univ. Arizona Press, Tucson, AZ, p. 539
Moudens A., Mousis O., Petit J.-M., Wurm G., Cordier D., Charnoz S., 2011, A&A, 531, A106
Oliveira I. et al., 2010, ApJ, 714, 778
Oliveira I., Olofsson J., Pontoppidan K. M., van Dishoeck E. F., Augereau J.-C., Merín B., 2011, ApJ, 734, 51
Pedersen A., Ines Gómez de Castro A., 2011, ApJ, 740, 77
Pinte C., Ménard F., Berger J. P., Benisty M., Malbet F., 2008, ApJ, 673, L63
Sargent B. A. et al., 2009, ApJS, 182, 477
Shakura N. I., Sunyaev R. A., 1973, A&A, 24, 337
Takeuchi T., Lin D. N. C., 2003, ApJ, 593, 524
Tannirkulam A., Harries T. J., Monnier J. D., 2007, ApJ, 661, 374
Tannirkulam A. et al., 2008, ApJ, 689, 513
Thi W.-F., Woitke P., Kamp I., 2011, MNRAS, 412, 711
Turner N. J., Carballido A., Sano T., 2010, ApJ, 708, 188
van Boekel R. et al., 2004, Nat, 432, 479
van Boekel R., Min M., Waters L. B. F. M., de Koter A., Dominik C., van den Ancker M. E., Bouwman J., 2005, A&A, 437, 189
Vinković D., 2003, PhD thesis, Univ. Kentucky
Vinković D., 2006, ApJ, 651, 906
Vinković D., 2009, Nat, 459, 227
Vinković D., Ivezić Ž., Miroshnichenko A. S., Elitzur M., 2003, MNRAS, 346, 1151
Vinković D., Ivezić Ž., Jurkić T., Elitzur M., 2006, ApJ, 636, 348
Watson D. M. et al., 2009, ApJS, 180, 84
Watson A. M., Stapelfeldt K. R., Wood K., Ménard F., 2007, in Reipurth B., Jewitt D., Keil K., eds, Protostars and Planets V. Univ. Arizona Press, Tucson, AZ, p. 523
Williams J. P., Cieza L. A., 2011, ARA&A, 49, 67

This paper has been typeset from a TEX/LATEX file prepared by the author.